Quantum Reissner-Nordström geometry: Singularity and Cauchy horizon

Roberto Casadio[1,2,*], Andrea Giusti[3,†] and Jorge Ovalle[4,5,‡]

[1]*Dipartimento di Fisica e Astronomia, Università di Bologna, via Irnerio 46, 40126 Bologna, Italy*
[2]*I.N.F.N., Sezione di Bologna, I.S. FLAG, viale B. Pichat 6/2, 40127 Bologna, Italy*
[3]*Institute for Theoretical Physics, ETH Zurich, Wolfgang-Pauli-Strasse 27, 8093 Zurich, Switzerland*
[4]*Research Centre of Theoretical Physics and Astrophysics Institute of Physics,*
Silesian University in Opava, CZ-746 01 Opava, Czech Republic
[5]*Departamento de Fısica, Facultad de Ciencias Básicas, Universidad de Antofagasta,*
Aptdo 02800, Antofagasta, Chile

We present a quantum description of electrically charged spherically symmetric black holes given by coherent states of gravitons in which both the central singularity and the Cauchy horizon are not realized.

I. INTRODUCTION AND MOTIVATION

Classical black hole solutions of general relativity contain spacetime singularities [1], which are expected to be removed in the quantum theory of the gravitational collapse of a compact source (see, e.g., Refs. [2]). Moreover, charged and rotating classical black holes also contain an inner Cauchy horizon, which signals a potential loss of predictability and also gives rise to mass inflation at the perturbative level (see, e.g., Refs. [3]). These latter considerations are the underlying motivations for the *strong cosmic censorship* conjecture [4,5], which can be simply phrased as the fact that the evolution of some sufficiently regular initial data should always give rise to a globally hyperbolic spacetime [6]. In particular, this conjecture implies that perturbations of the inner Cauchy horizon should turn it into a curvature singularity.

Quite interestingly, many candidates as regular black holes appearing in the literature (for an incomplete list, see Refs. [7]) also display a inner horizon (with some interesting exceptions, like those in Refs. [8]). One might then wonder if trading the central singularity for a Cauchy horizon represents a real progress in our understanding of black hole physics. More generally, one would like to understand how regular the geometry really needs to be for physical consistency and whether this trade-off can be avoided. In this respect, it is also interesting to note that the inner horizon that forms in models of gravitational collapse [2] is not eternal. Therefore, a regular black hole with an inner horizon generated by the gravitational collapse does not necessarily have (lasting) issues concerning the initial value problem, or the instabilities associated with Cauchy horizons. On the other hand, there is no guarantee that these issues are always avoided in collapse models and one must check on a case by case basis.

In Ref. [9], a quantum coherent state for the spherically symmetric and electrically neutral Schwarzschild metric was introduced, following ideas from Refs. [10–13]. This coherent state is built for a scalar field, which in turn is meant to effectively describe the geometry itself as a gravitational potential emerging from the (longitudinal or temporal) polarizations of the graviton. It was in particular shown in Ref. [9] that the conditions for the very existence of such a quantum state require departures from the purely classical behavior both in the infrared (IR) and, more importantly, in the ultraviolet (UV). The IR behavior can be connected with the finite extent of our causally connected Universe [14]. The UV deviation from the classical general relativistic vacuum can instead be interpreted as the existence of a (quantum) extended matter core, which sources the geometry [15] and gives rise to quantum hair [16,17]. This quantum core indeed removes the central singularity and keeps tidal forces everywhere finite. Geometrical quantities like the Ricci curvature and the Kretschmann scalar still diverge toward the origin, but their integrals remain finite, which corresponds to having a so-called integrable singularity. Furthermore, no inner horizon appears for any size of the matter core.

In order to investigate the causal structure of spherically symmetric quantum black holes with electric charge, in this work we apply the approach of Ref. [9] to the Reissner-Nordström metric

$$ds^2 = -(1 + 2V_{RN})dt^2 + \frac{dr^2}{1 + 2V_{RN}} + r^2 d\Omega^2, \quad (1.1)$$

[*]casadio@bo.infn.it
[†]agiusti@phys.ethz.ch
[‡]jorge.ovalle@physics.slu.cz

with[1]

$$V_{RN} = -\frac{G_N M}{r} + \frac{G_N Q^2}{2r^2} \equiv V_M + V_Q, \qquad (1.2)$$

where M is the ADM mass [18] and Q the charge of the black hole. We recall that, for $G_N M^2 > Q^2$, the above spacetime contains two horizons determined by $g^{rr} = 1 + 2V_{RN} = 0$, namely

$$R_{\pm} = G_N M \pm \sqrt{G_N^2 M^2 - G_N Q^2}, \qquad (1.3)$$

with R_+ being the event horizon and R_- a Cauchy horizon. The quantum version of the functions V_M and V_Q in Eq. (1.2) will be employed in order to reconstruct a quantum corrected complete metric to replace (1.1). From this new metric, one can then analyze how the necessary material core predicted by quantum physics affects the singularity, inner horizon and thermodynamics. In particular, we assume that it is in this core that resides the charge Q.

In Sec. II, we will derive in details the coherent state for the metric (1.1) and the corresponding quantum metric will then be analyzed in Sec. III; concluding remarks and outlooks will be provided in Sec. IV.

II. QUANTUM COHERENT STATE FOR THE REISSNER-NORDSTRÖM GEOMETRY

Following Ref. [9], we assume that the quantum vacuum $|0\rangle$ corresponds to a spacetime devoid of any matter or gravitational excitations. In order to effectively describe the gravitational excitations giving rise to the geometry, we first rescale the potential V_{RN} so as to obtain a canonically normalized real scalar field $\Phi = \sqrt{m_p/\ell_p} V_{RN}$, and then quantize Φ as a massless field satisfying the free wave equation in the Minkowski spacetime

$$\left[-\frac{\partial^2}{\partial t^2} + \frac{1}{r^2} \frac{\partial}{\partial r} \left(r^2 \frac{\partial}{\partial r} \right) \right] \Phi(t, r) = 0. \qquad (2.1)$$

Since we are only interested in static configurations, it is convenient to choose the normal modes of Eq. (2.1) described in terms of spherical Bessel functions $j_0 = \sin(kr)/kr$ for $k > 0$, that is

$$u_k(t, r) = e^{-ikt} j_0(kr). \qquad (2.2)$$

The quantum field operator,

$$\hat{\Phi}(t, r) = \int_0^\infty \frac{k^2 dk}{2\pi^2} \sqrt{\frac{\hbar}{2k}} [\hat{a}_k u_k(t, r) + \hat{a}_k^\dagger u_k^*(t, r)], \qquad (2.3)$$

and its conjugate momentum,

$$\hat{\Pi}(t, r) = i \int_0^\infty \frac{k^2 dk}{2\pi^2} \sqrt{\frac{\hbar k}{2}} [\hat{a}_k u_k(t, r) - \hat{a}_k^\dagger u_k^*(t, r)], \qquad (2.4)$$

satisfy the equal time commutation relations,

$$[\hat{\Phi}(t, r), \hat{\Pi}(t, s)] = \frac{i\hbar}{4\pi r^2} \delta(r - s), \qquad (2.5)$$

if

$$[\hat{a}_k, \hat{a}_p^\dagger] = \frac{2\pi^2}{k^2} \delta(k - p). \qquad (2.6)$$

The Fock space is then built from the vacuum defined by $\hat{a}_k |0\rangle = 0$ for all $k > 0$.

The classical static configurations (1.2) are realized in the quantum theory as coherent states $|g\rangle$ such that $\hat{a}_k |g\rangle = g(k) e^{i\gamma_k(t)} |g\rangle$ and

$$\sqrt{\frac{\ell_p}{m_p}} \langle g | \hat{\Phi}(t, r) | g \rangle = V_{RN}(r). \qquad (2.7)$$

From the expansion (2.3), we obtain

$$\langle g | \hat{\Phi}(t, r) | g \rangle = \int_0^\infty \frac{k^2 dk}{2\pi^2} \sqrt{\frac{2\ell_p m_p}{k}} g(k) \cos[\gamma_k(t) - kt] j_0(kr), \qquad (2.8)$$

and time-independence is obtained by setting $\gamma_k = kt$.[2] If we write the classical potential as

$$V_{RN} = \int_0^\infty \frac{k^2 dk}{2\pi^2} [\tilde{V}_M(k) + \tilde{V}_Q(k)] j_0(kr), \qquad (2.9)$$

we obtain

$$\tilde{V}_M = -4\pi G_N \frac{M}{k^2} \qquad (2.10)$$

and

---

[1]We shall use units with $c = 1/4\pi\epsilon_0 = 1$, $G_N = \ell_p/m_p$, $\hbar = \ell_p m_p$, with ℓ_p the Planck length and m_p the Planck mass. Hence, the combination $G_N Q^2$ has dimensions of a length squared.

[2]We recall that static potentials are obtained from nonpropagating modes in quantum field theory [12,13,19].

$$\tilde{V}_Q = \pi^2 G_{\mathrm{N}} \frac{Q^2}{k}. \tag{2.11}$$

The coherent state is thus determined by the occupation numbers

$$g_M(k) = \sqrt{\frac{k}{2} \frac{\tilde{V}_M}{\ell_{\mathrm{p}}}} = -\frac{4\pi M}{\sqrt{2k^3} m_{\mathrm{p}}} \tag{2.12}$$

and

$$g_Q(k) = \sqrt{\frac{k}{2} \frac{\tilde{V}_Q}{\ell_{\mathrm{p}}}} = \frac{\pi^2 Q^2}{\sqrt{2k} m_{\mathrm{p}}}, \tag{2.13}$$

and it finally reads

$$|g\rangle = e^{-N_{\mathrm{G}}/2} \exp\left\{ \int_0^\infty \frac{k^2 \mathrm{d}k}{2\pi^2} [g_M(k) + g_Q(k)] \hat{a}_k^\dagger \right\} |0\rangle, \tag{2.14}$$

where the total occupation number is given by

$$N_{\mathrm{G}} = \int_0^\infty \frac{k^2 \mathrm{d}k}{2\pi^2} [g_M(k) + g_Q(k)]^2$$

$$\equiv N_M + N_Q + N_{MQ}. \tag{2.15}$$

In particular, the contribution N_M associated with the ADM mass M is the same as the one for the Schwarzschild metric [9] and diverges for the exact occupation numbers g_M given in Eq. (2.12). This divergence implies that the $g_M = g_M(k)$ which are realized in Nature must have different IR and UV behaviors, and that the corresponding metric must therefore differ from the classical expression.

Assuming that we do not know the actual quantum states which are realized in Nature, we can formally express the requirement that the state $|g\rangle$ is well defined by introducing (sharp) IR and UV cutoffs $k_{\mathrm{IR}} \sim R_\infty^{-1}$ and $k_{\mathrm{UV}} \sim R_{\mathrm{UV}}^{-1}$, with $R_{\mathrm{UV}} < R_+ \ll R_\infty$. It is then important to remark that the specific functional dependences on R_∞ and R_{UV} displayed in the following are consequences of the choice of sharp cutoffs in the momentum integrals and should not be taken too literally. With this proviso, one finds

$$N_M = \frac{4M^2}{m_{\mathrm{p}}^2} \int_{k_{\mathrm{IR}}}^{k_{\mathrm{UV}}} \frac{\mathrm{d}k}{k} = \frac{4M^2}{m_{\mathrm{p}}^2} \ln\left(\frac{R_\infty}{R_{\mathrm{UV}}}\right). \tag{2.16}$$

Likewise, we have

$$N_Q = \frac{\pi^2 Q^4}{4 m_{\mathrm{p}}^2} \int_{k_{\mathrm{IR}}}^{k_{\mathrm{UV}}} k \mathrm{d}k = \frac{\pi^2 Q^4}{8 m_{\mathrm{p}}^2} \left(\frac{1}{R_{\mathrm{UV}}^2} - \frac{1}{R_\infty^2}\right) \tag{2.17}$$

and the cross term

$$N_{MQ} = -\frac{2\pi M Q^2}{m_{\mathrm{p}}^2} \int_{k_{\mathrm{IR}}}^{k_{\mathrm{UV}}} \mathrm{d}k = -\frac{2\pi M Q^2}{m_{\mathrm{p}}^2} \left(\frac{1}{R_{\mathrm{UV}}} - \frac{1}{R_\infty}\right). \tag{2.18}$$

Another quantity of interest is the average radial momentum

$$\langle k \rangle = \int_0^\infty \frac{k^2 \mathrm{d}k}{2\pi^2} k [g_M(k) + g_Q(k)]^2$$

$$\equiv \langle k \rangle_M + \langle k \rangle_Q + \langle k \rangle_{MQ}, \tag{2.19}$$

where the mass contribution is given by

$$\langle k \rangle_M = \frac{4M^2}{m_{\mathrm{p}}^2} \int_{k_{\mathrm{IR}}}^{k_{\mathrm{UV}}} \mathrm{d}k = \frac{4M^2}{m_{\mathrm{p}}^2} \left(\frac{1}{R_{\mathrm{UV}}} - \frac{1}{R_\infty}\right), \tag{2.20}$$

the charge contribution by

$$\langle k \rangle_Q = \frac{\pi^2 Q^4}{4 m_{\mathrm{p}}^2} \int_{k_{\mathrm{IR}}}^{k_{\mathrm{UV}}} k^2 \mathrm{d}k = \frac{\pi^2 Q^4}{12 m_{\mathrm{p}}^2} \left(\frac{1}{R_{\mathrm{UV}}^3} - \frac{1}{R_\infty^3}\right) \tag{2.21}$$

and the cross term by

$$\langle k \rangle_{MQ} = -\frac{\pi M Q^2}{m_{\mathrm{p}}^2} \int_{k_{\mathrm{IR}}}^{k_{\mathrm{UV}}} k \mathrm{d}k$$

$$= -\frac{\pi M Q^2}{m_{\mathrm{p}}^2} \left(\frac{1}{R_{\mathrm{UV}}^2} - \frac{1}{R_\infty^2}\right). \tag{2.22}$$

From the above results, one can obtain the "typical" wavelength λ_{G}. Specifically, assuming $R_\infty \gg R_{\mathrm{UV}}$, one finds at leading order

$$N_{\mathrm{G}} \simeq \frac{4M^2}{m_{\mathrm{p}}^2} \ln\left(\frac{R_\infty}{R_{\mathrm{UV}}}\right) + \frac{\pi^2 Q^4}{8 m_{\mathrm{p}}^2 R_{\mathrm{UV}}^2} - \frac{2\pi M Q^2}{m_{\mathrm{p}}^2 R_{\mathrm{UV}}} \tag{2.23}$$

and

$$\langle k \rangle \simeq \frac{4M^2}{m_{\mathrm{p}}^2 R_{\mathrm{UV}}} + \frac{\pi^2 Q^4}{12 m_{\mathrm{p}}^2 R_{\mathrm{UV}}^3} - \frac{\pi M Q^2}{m_{\mathrm{p}}^2 R_{\mathrm{UV}}^2}. \tag{2.24}$$

If we further assume $2 G_{\mathrm{N}} M \gg G_{\mathrm{N}} Q^2$, we find the approximate expression

$$\lambda_{\mathrm{G}} = \frac{N_{\mathrm{G}}}{\langle k \rangle} \simeq R_{\mathrm{UV}} \left(1 + \frac{\pi Q^2}{4 M R_{\mathrm{UV}}}\right) \ln\left(\frac{R_\infty}{R_{\mathrm{UV}}}\right), \tag{2.25}$$
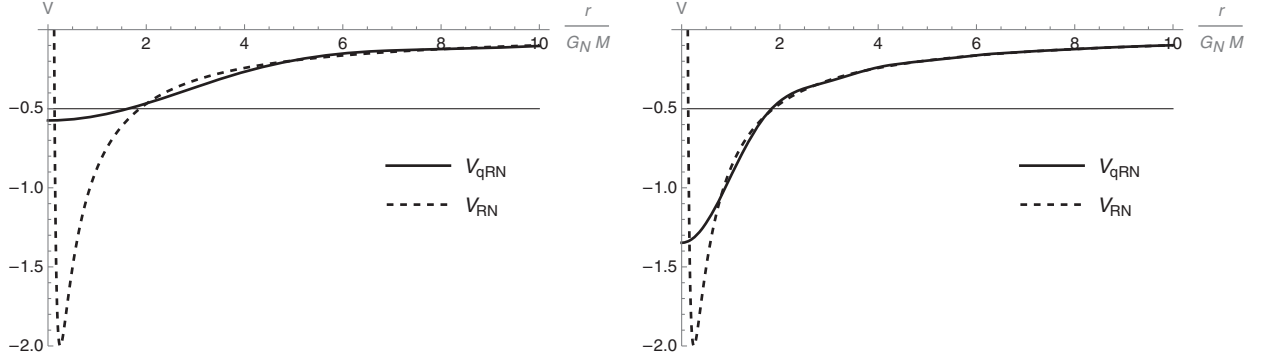
FIG. 1.   Quantum potential V_{qRN} in Eq. (3.3) (solid line) compared to V_{RN} (dashed line) for $R_{UV} = G_N M = 2\sqrt{G_N Q^2}$ (left panel) and for $R_{UV} = G_N M/3 = 2\sqrt{G_N Q^2}/3$ (right panel). The thin solid line $V = -1/2$ crosses the potential at the horizons.

which reduces to the Schwarzschild case [9] for $Q = 0$. The effect of (a relatively small) charge is therefore to increase the typical wavelength of the gravitons building the geometry.

III. QUANTUM CORRECTED REISSNER-NORDSTRÖM SPACETIME

We can now reconstruct the quantum corrected metric functions by simply integrating back the occupation numbers (2.12) and (2.13) between the IR and UV cutoffs, which yields

$$V_{qM} = -\frac{2G_N M}{\pi r}\left[\text{Si}\left(\frac{r}{R_{UV}}\right) - \text{Si}\left(\frac{r}{R_\infty}\right)\right], \quad (3.1)$$

where $\text{Si} = \text{Si}(x)$ denotes the sine integral function, and

$$V_{qQ} = \frac{G_N Q^2}{2r^2}\left[\cos\left(\frac{r}{R_\infty}\right) - \cos\left(\frac{r}{R_{UV}}\right)\right]. \quad (3.2)$$

In both expressions, we can safely take the limit $R_\infty \to \infty$ as an approximation, so that we finally obtain

$$V_{qRN} \simeq -\frac{2G_N M}{\pi r}\text{Si}\left(\frac{r}{R_{UV}}\right) + \frac{G_N Q^2}{2r^2}\left[1 - \cos\left(\frac{r}{R_{UV}}\right)\right]. \quad (3.3)$$

Two examples of the corrected potential are plotted in Fig. 1. We can in particular notice that the oscillations around the classical mass contribution asymptote to zero,[3] whereas the oscillations around the term containing the charge Q have constant amplitude (see Fig. 2).

---

[3]We recall that $\lim_{x\to\infty}\text{Si}(x) = \pi/2$.

We next use the function (3.3) to define the quantum corrected metric

$$ds^2 \simeq -(1 + 2V_{qRN})dt^2 + \frac{dr^2}{1 + 2V_{qRN}} + r^2 d\Omega^2, \quad (3.4)$$

where the approximate equality is to remind us of all the simplifying assumptions, including the fact that we have neglected the IR departure from the classical behavior. Strictly speaking, the above approximation is valid as long as we consider $R_{UV} \ll r \ll R_\infty$. Nonetheless, we will investigate the entire region $r > 0$ in the following.

A. Effective source

From the point of view of general relativity, both the classical Reissner-Nordström metric (1.1) and Eq. (3.4) are not solutions in the vacuum. The (effective) Einstein equations are sourced by an (effective) energy-momentum tensor

$$T^\mu{}_\nu = \text{diag}(-\rho^{\text{eff}}, p_r^{\text{eff}}, p_t^{\text{eff}}, p_t^{\text{eff}}) = \frac{G^\mu{}_\nu}{8\pi G_N}. \quad (3.5)$$

One can then compute the Einstein tensor $G_{\mu\nu}$ for the metric (3.4) in order to determine the effective energy density

$$\rho^{\text{eff}} = \frac{Q^2}{8\pi r^4}\left[1 - \cos\left(\frac{r}{R_{UV}}\right)\right] + \frac{4MR_{UV} - \pi Q^2}{8\pi^2 r^3 R_{UV}}\sin\left(\frac{r}{R_{UV}}\right) \quad (3.6)$$

the radial pressure

$$p_r^{\text{eff}} = -\rho^{\text{eff}}, \quad (3.7)$$

and the tension

$$p_t^{\text{eff}} = \frac{Q^2}{8\pi r^4}\left[1 - \cos\left(\frac{r}{R_{\text{UV}}}\right)\right] + \frac{(\pi Q^2 - 4MR_{\text{UV}})r\cos(\frac{r}{R_{\text{UV}}}) + 2R_{\text{UV}}(2MR_{\text{UV}} - \pi Q^2)\sin(\frac{r}{R_{\text{UV}}})}{16\pi^2 r^3 R_{\text{UV}}^2}. \tag{3.8}$$

In the above expressions, the first term (independent of the cutoff R_{UV}) is the standard (traceless) electrostatic contribution for the Reissner-Nordström metric,

$$\rho^{\text{RN}} = -p_r^{\text{RN}} = p_t^{\text{RN}} = \frac{Q^2}{8\pi r^4}. \tag{3.9}$$

The additional terms in Eq. (3.6),

$$\rho^{\text{eff}} - \rho^{\text{RN}} = \frac{M}{2\pi^2 r^3}\sin\left(\frac{r}{R_{\text{UV}}}\right)$$
$$- \frac{Q^2}{8\pi r^4}\left[\cos\left(\frac{r}{R_{\text{UV}}}\right) + \frac{r}{R_{\text{UV}}}\sin\left(\frac{r}{R_{\text{UV}}}\right)\right], \tag{3.10}$$

and those in Eq. (3.8),

$$p_t^{\text{eff}} - p_t^{\text{RN}} = \frac{M}{4\pi^2 r^3}\left[\sin\left(\frac{r}{R_{\text{UV}}}\right) - \frac{r}{R_{\text{UV}}}\cos\left(\frac{r}{R_{\text{UV}}}\right)\right]$$
$$- \frac{Q^2}{8\pi r^4}\left[\left(1 - \frac{r^2}{2R_{\text{UV}}^2}\right)\cos\left(\frac{r}{R_{\text{UV}}}\right)\right.$$
$$\left. + \frac{r}{R_{\text{UV}}}\sin\left(\frac{r}{R_{\text{UV}}}\right)\right], \tag{3.11}$$

can therefore be interpreted as representing an effective (quantum) smearing of both the mass and the charge of the central source over the length scale R_{UV}. The energy density and pressures corresponding to the cases in Figs. 1 and 2 are displayed in Figs. 3 and 4.

The energy-momentum tensor (3.5) satisfies the conservation equation $\nabla_\mu T^{\mu\nu} = 0$ by construction. In particular, the only nontrivial condition is for $\nu = 1$ and yields the Tolman-Oppenheimer-Volkoff (TOV) equation
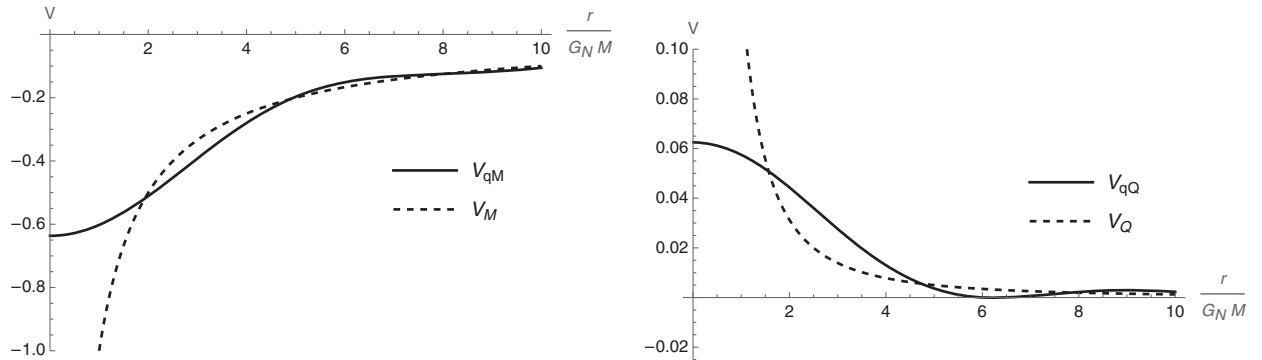

FIG. 2. Quantum potential V_{qM} in Eq. (3.1) (solid line) compared to V_M (dashed line) for $R_{\text{UV}} = G_N M = 2\sqrt{G_N Q^2}$ (left panel) and V_{qQ} in Eq. (3.2) (solid line) compared to V_Q for $R_{\text{UV}} = G_N M/3 = 2\sqrt{G_N Q^2}/3$ (right panel).
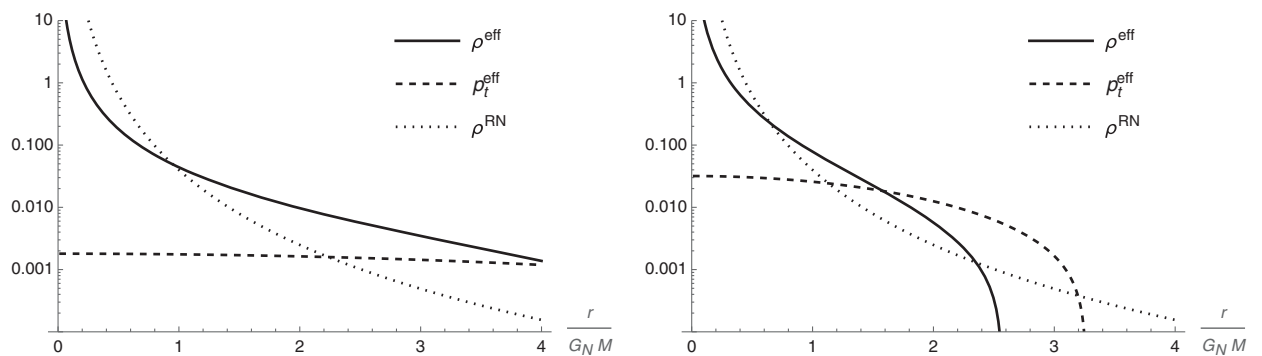

FIG. 3. Effective energy density (solid line) and tangential pressure (dashed line) in Eq. (3.5) compared to the Reissner-Nordström contribution (3.9) (dotted line) for $R_{\text{UV}} = G_N M = 2\sqrt{G_N Q^2}$ (left panel) and for $R_{\text{UV}} = G_N M/3 = 2\sqrt{G_N Q^2}/3$ (right panel).
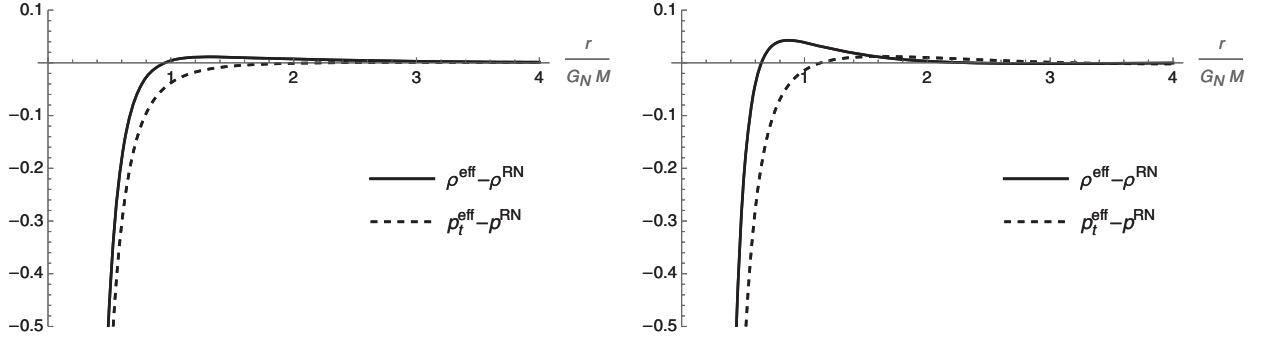
FIG. 4. Quantum contribution to the effective energy density (solid line) and tangential pressure (dashed line) in Eq. (3.5) for $R_{\rm UV} = G_{\rm N}M = 2\sqrt{G_{\rm N}Q^2}$ (left panel) and for $R_{\rm UV} = G_{\rm N}M/3 = 2\sqrt{G_{\rm N}Q^2}/3$ (right panel).

$$\frac{dp_r^{\rm eff}}{dr} = -\frac{1}{1 + 2V_{\rm qRN}}\frac{dV_{\rm qRN}}{dr}(\rho^{\rm eff} + p_r^{\rm eff}) + \frac{2}{r}(p_t^{\rm eff} - p_r^{\rm eff}),$$

$$(3.12)$$

which governs the hydrodynamic equilibrium of the system. In particular, the quantum corrected metric (3.4) is still of the Kerr-Schild form [20], and the effective fluid is anisotropic with $p_t^{\rm eff} \neq p_r^{\rm eff}$. We can then note that the metric (3.4) can be formally thought as the coupling [21,22] of two mass functions in a Kerr-Schild spacetime, namely

$$\tilde{m} = m_{\rm RN} + m_{\rm q}, \qquad (3.13)$$

where the mass function of the Reissner-Nordström solution is given by

$$m_{\rm RN} = M - \frac{Q^2}{2r}, \qquad (3.14)$$

while

$$m_{\rm q} = M\left[\frac{2}{\pi}{\rm Si}\left(\frac{r}{R_{\rm UV}}\right) - 1\right] + \frac{Q^2}{2r}\cos\left(\frac{r}{R_{\rm UV}}\right) \qquad (3.15)$$

is the mass function of the effective quantum fluid filling the spacetime (see Fig. 5).

We next proceed to study the causal structure of the quantum corrected metric.

B. Singularity

We can start by analyzing the metric (3.4) near $r = 0$. In particular, we find

$$V_{\rm qRN}(0) = \frac{G_{\rm N}(\pi Q^2 - 8MR_{\rm UV})}{4\pi R_{\rm UV}^2} \qquad (3.16)$$

and

$$\left.\frac{dV_{\rm qRN}}{dr}\right|_{r=0} = 0, \qquad (3.17)$$

from which we expect no central singularity. In fact, we can compute the Ricci scalar to leading order around $r = 0$,

$$R \simeq \frac{G_{\rm N}(8MR_{\rm UV} - \pi Q^2)}{\pi R_{\rm UV}^2 r^2} \sim -\frac{V_{\rm qRN}(0)}{r^2} \qquad (3.18)$$

and the Kretschmann scalar

$$R_{\alpha\beta\mu\nu}R^{\alpha\beta\mu\nu} \simeq R^2 \sim r^{-4}. \qquad (3.19)$$

The center of the system is therefore an integrable singularity [23] where tidal forces remain finite and the volume integral of the Ricci scalar is also finite. This is to be compared with the standard results $R^2 \sim R_{\alpha\beta\mu\nu}R^{\alpha\beta\mu\nu} \sim Q^4/r^8$ for the Reissner-Nordström metric (1.1).

The fact that the origin is regular is further supported by the expressions of the energy density for $r \sim 0$, that is

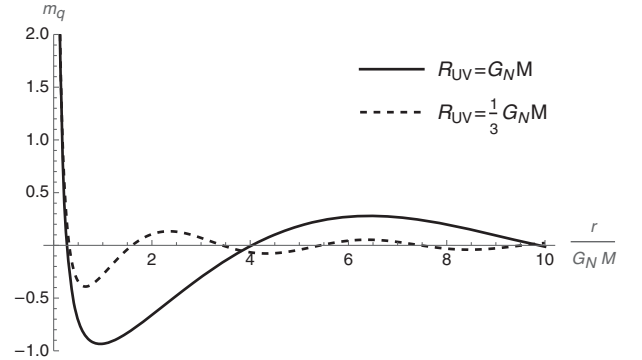$$\rho^{\rm eff} = -p_r^{\rm eff} \simeq \frac{8MR_{\rm UV} - \pi Q^2}{16\pi^2 r^2 R_{\rm UV}^2}, \qquad (3.20)$$

FIG. 5. Mass function in Eq. (3.15) for $R_{\rm UV} = G_{\rm N}M = 2\sqrt{G_{\rm N}Q^2}$ (solid line) and for $R_{\rm UV} = G_{\rm N}M/3 = 2\sqrt{G_{\rm N}Q^2}/3$ (dashed line).

and the analog expression for the tension

$$p_t^{\text{eff}} \simeq \frac{16MR_{\text{UV}} - 3\pi Q^2}{192\pi^2 R_{\text{UV}}^4}. \qquad (3.21)$$

Many regular black holes violate some energy conditions for $r \sim 0$ [7]. However, from Eqs. (3.20) and (3.21), we can see that for

$$16MR_{\text{UV}} \geq 3\pi Q^2, \qquad (3.22)$$

the strong energy condition is satisfied.

C. Event and Cauchy horizons

The metric (3.4) can contain horizons determined by

$$g^{rr} = -g_{tt} = 1 + 2V_{\text{qRN}} = 0, \qquad (3.23)$$

the largest zero being the event horizon $R_{\text{q+}}$ analogous to R_+ in Eq. (1.3). It is not possible to find analytical expressions for the above zeros for general values of M, Q and R_{UV} (see also Appendix). A simple numerical

inspection shows that $R_{\text{q+}}$ exists in general if $R_{\text{UV}} \lesssim R_+$ and Q^2 is such that $R_- \ll R_+$. We are then particularly interested in the existence of the inner Cauchy horizon, that is a second zero $R_{\text{q-}} < R_{\text{q+}}$, when the event horizon $R_{\text{q+}}$ also exists. Again, a simple numerical analysis shows that no Cauchy horizon exists if $R_- \lesssim R_{\text{UV}} \lesssim R_+$, whereas there can be a inner horizon for $R_{\text{UV}} \lesssim R_-$ (see left and right panels in Fig. 6, respectively). In Fig. 7 we also show that there is no event horizon for $R_{\text{UV}} \gtrsim R_+$ (left panel) and there can be multiple inner horizons for $R_{\text{UV}} \ll R_-$ (right panel). Since there is no central singularity, the former case would represent an electrically charged star.

The quantum corrected causal structure for $R_- \lesssim R_{\text{UV}} \lesssim R_+$ is in qualitative agreement with the quantum mechanical description of the gravitational radius in Ref. [24], where the probability of finding the matter source inside the inner Cauchy horizon R_- was shown to be small for masses above the Planck scale and charge Q sufficiently below extremality. One can then consider values of M and Q near the classical extremal case $R_+ = R_-$, that is $Q^2 \simeq G_N M^2$ [25]. Figure 8 shows two examples of extremal geometries for different values of the
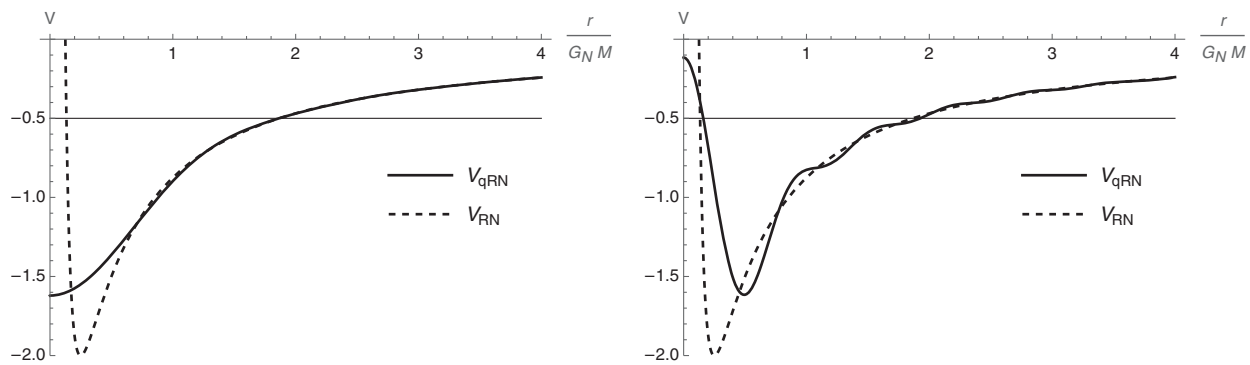

FIG. 6. Quantum potential V_{qRN} in Eq. (3.3) (solid line) compared to V_{RN} (dashed line) for $R_{\text{UV}} = G_N M/5 = 2\sqrt{G_N Q^2}/5 > R_- \simeq 0.13 G_N M$ (left panel) and for $R_{\text{UV}} = G_N M/10 = \sqrt{G_N Q^2}/5 < R_-$ (right panel). The thin solid line $V = -1/2$ crosses the potential at the horizons.

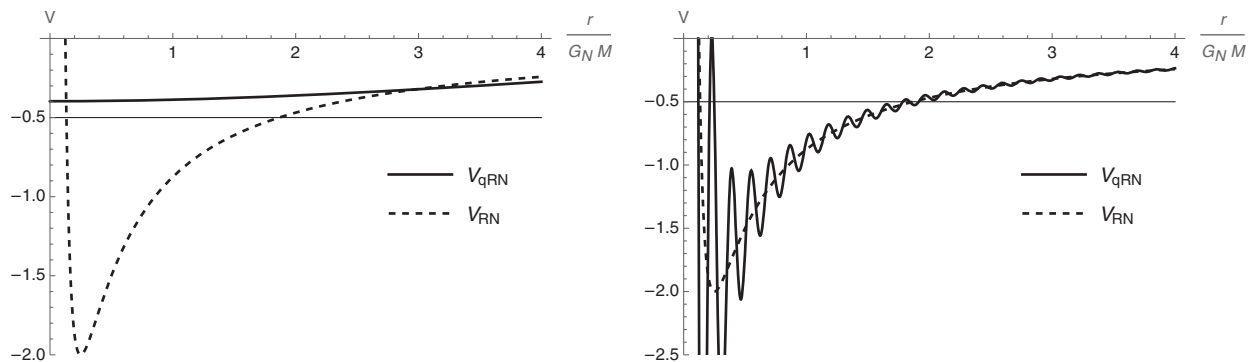FIG. 7. Quantum potential V_{qRN} in Eq. (3.3) (solid line) compared to V_{RN} (dashed line) for $R_{\text{UV}} = 3G_N M/2 = 3\sqrt{G_N Q^2} \simeq R_+ \simeq 1.8 G_N M$ (left panel) and for $R_{\text{UV}} = G_N M/50 = \sqrt{G_N Q^2}/25 \ll R_- \simeq 0.13 G_N M$ (right panel). The thin solid line $V = -1/2$ crosses the potential at the horizons.
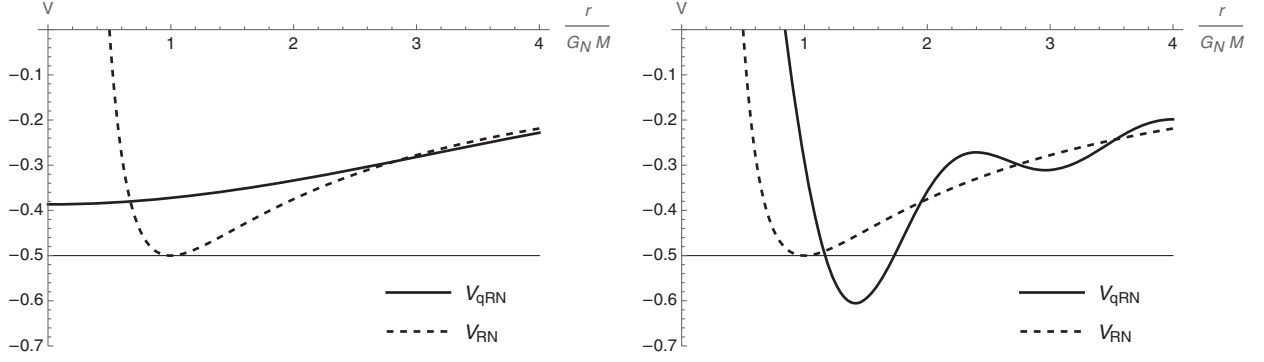
FIG. 8. Quantum potential V_{qRN} in Eq. (3.3) (solid line) compared to V_{RN} (dashed line) for the extremal case $R_- = R_+$ with $R_{UV} = R_+$ (left panel) and $R_{UV} = R_+/4$ (right panel). The thin solid line $V = -1/2$ crosses the potential at the horizon.

scale R_{UV}. For $R_{UV} \gtrsim R_+$, the geometry is regular everywhere, with no horizons and no singularity. If one lets R_{UV} fall below R_+, one in general obtains two (or more) horizons. For a given $|Q| = \sqrt{G_N}M$, one can fine-tune R_{UV} so that one degenerate horizon exists like in the classical case, but such a value can only be determined numerically (see Appendix).

For $Q^2 > G_N M^2$, the classical Reissner-Nordström geometry becomes a naked singularity. We show an example of the corresponding quantum corrected metric in Fig. 9. For $R_{UV} \gtrsim G_N M$, one again obtains a regular geometry, whereas for $R_{UV} \lesssim G_N M$ a varying number of horizons in general reappears. In this case, one can therefore have either a regular distribution of matter and charge, or a regular black hole. Like for the extremal case discussed above, the value of R_{UV} that separates the two different behaviors can only be determined numerically for given M and Q.

D. Thermodynamics

We recall that the Bekenstein-Hawking entropy is simply given by the area law [26]

$$S_{qRN} = \frac{\mathcal{A}_H}{4\ell_p^2} = \frac{\pi R_{q+}^2}{\ell_p^2} \qquad (3.24)$$
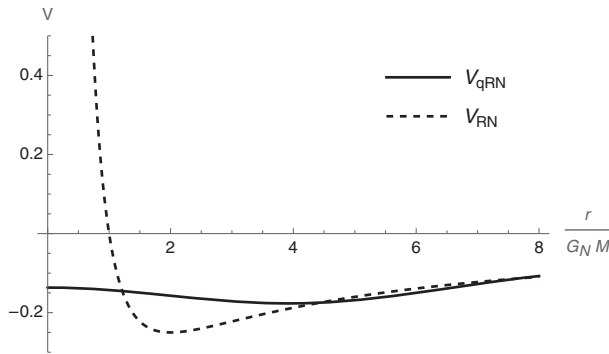
and the black hole temperature [27]

$$T_{qRN} = \frac{\hbar \kappa_{qRN}}{2\pi} = \frac{\hbar}{2\pi} \frac{dV_{qRN}}{dr}\bigg|_{r=R_{q+}}, \qquad (3.25)$$

where κ is the surface gravity at the horizon. Unfortunately, none of the above expressions can be computed analytically, because R_{q+} can only be estimated numerically.

For M and Q such that $R_- \lesssim R_{UV} \lesssim R_+$, like the left panel in Fig. 6, deviations from the classical metric become very small and one therefore expects just small numerical differences with respect to the classical expressions, that is

$$S_{qRN} \simeq S_{RN} = \frac{\pi R_+^2}{\ell_p^2} \qquad (3.26)$$

and

$$\kappa_{qRN} \simeq \kappa_{RN} = \frac{G_N(MR_+ - Q^2)}{R_+^3}, \qquad (3.27)$$

where R_+ is given in Eq. (1.3).

Much larger deviations are expected for $R_{UV} \simeq R_+$, for which the quantum corrected event horizon become much
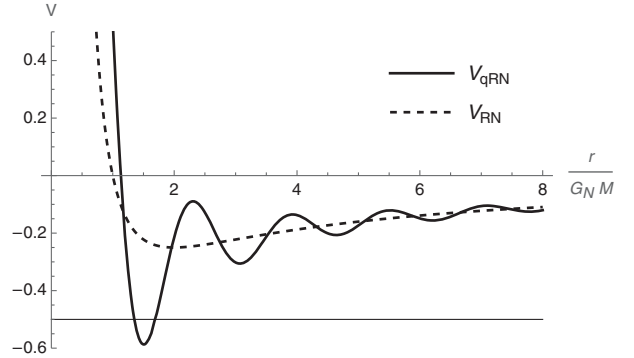

FIG. 9. Quantum potential V_{qRN} in Eq. (3.3) (solid line) compared to V_{RN} (dashed line) for classical naked singularity $\sqrt{G_N Q^2} = 2G_N M$ with $R_{UV} = G_N M$ (left panel) and $R_{UV} = G_N M/4$ (right panel). The thin solid line $V = -1/2$ crosses the potential at the horizon.

smaller then R_+ or disappears (like in the left panel of Fig. 7).

IV. CONCLUSIONS AND OUTLOOK

General relativity predicts the existence of singularities, which appear in black hole solutions as the final product of the gravitational collapse. This represents a clear limitation of the theory, and presumably its quantum version should cure these pathologies. Regular black holes represent simple workarounds to the problem of curvature singularity that allow one to remain within the geometric description of general relativity, thus without resorting to any quantum argument. However, these solutions often suffer of several caveats. First, the matter distribution that generates these geometries has to violate the various energy conditions that are typically ascribed to standard matter. Nonetheless, such a scenario can be regarded as a mere effective description of a system in a fully quantum regime, for which we still lack a proper UV description. Second, and most importantly, such regular solutions typically entail the existence of inner Cauchy horizons, signalling a breakdown of predictability.

Starting from the idea that the classical geometry of a compact object should emerge from a suitable description of the quantum state of both gravity and matter, we have reconstructed a quantum-corrected Reissner-Nordström geometry. Such a geometry enjoys an integrable singularity, where tidal forces remain finite, and the absence of inner Cauchy horizons when the UV cutoff R_{UV} is such that $R_- \lesssim R_{UV} \lesssim R_+$. If the cutoff scale R_{UV} is associated with the final size of the collapsing object, it appears sensible that it will never shrink below the would-be inner horizon, and the latter is therefore avoided.

The same issues emerge in rotating black holes. In order to provide a quantum description for these more complex classical geometries, the approach from Ref. [9] employed here will have to be generalized, for example by using a procedure similar to the one in Ref. [28].

APPENDIX: MASS FUNCTION AND HORIZON RADIUS

In the standard Reissner-Nordström metric, one can trade the dependence on the ADM mass M for one of the zeros in Eq. (1.3) of the metric functions $g^{rr} = -g_{tt}$ by defining

$$f(r, Q) = \frac{G_N Q^2}{r^2}, \tag{A1}$$

and

$$g^{rr} = 1 - \frac{R_\pm}{r}[1 + f(R_\pm, Q)] + f(r, Q)$$
$$= 1 - \frac{R_\pm^2 + G_N Q^2}{R_\pm r} + \frac{G_N Q^2}{r^2}. \tag{A2}$$

The ADM mass is now given by

$$2G_N M = R_\pm[1 + f(R_\pm, Q)] = R_\pm\left(1 + \frac{G_N Q^2}{R_\pm^2}\right), \tag{A3}$$

which yields Eq. (1.3) as expected.

For the quantum corrected metric (3.4), it is easier to just solve Eq. (3.23) for the mass M as a function of a generic zero $r = r_H$, which yields

$$2G_N M = \frac{r_H + \frac{G_N Q^2}{r_H}[1 - \cos(\frac{r_H}{R_{UV}})]}{\frac{2}{\pi} \text{Si}(\frac{r_H}{R_{UV}})}. \tag{A4}$$

The metric function then reads

$$g^{rr} = 1 - \frac{\text{Si}(\frac{r}{R_{UV}})}{\text{Si}(\frac{r_H}{R_{UV}})}\left\{1 + \frac{G_N Q^2}{r_H^2}\left[1 - \cos\left(\frac{r_H}{R_{UV}}\right)\right]\right\}\frac{r_H}{r}$$
$$+ \frac{G_N Q^2}{r^2}\left[1 - \cos\left(\frac{r}{R_{UV}}\right)\right]. \tag{A5}$$

By studying the function (A4), one can in principle see for what values of M and Q there exists more values of r_H depending on R_{UV}. In practice, this analysis can only be performed numerically.
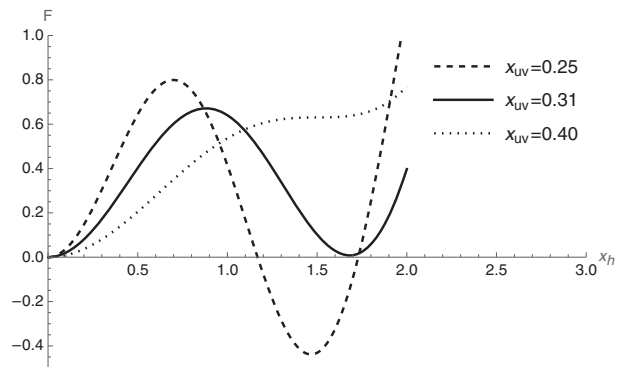

FIG. 10. The function F in Eq. (A6) shows the existence of two horizons for $x_s \simeq 0.25$ (dashed line), one degenerate horizon for $x_s \simeq 0.31$ (solid line) and no horizons for $x_s \simeq 0.40$ (dotted line).

For example, in the classical extremal case $Q^2 = G_N M^2$, Eq. (A3) simplifies to

$$F(x_h; x_s) \equiv x_h^2 - \frac{4}{\pi} x_h \mathrm{Si}\left(\frac{x_h}{x_s}\right) + 1 - \cos\left(\frac{x_h}{x_s}\right) = 0, \quad (A6)$$

where we defined $x_h \equiv r_H / G_N M$ and $x_{uv} \equiv R_{UV} / G_N M$. Figure 10 shows the function F for three different values of x_s corresponding to geometries with two horizons, one degenerate horizon and no horizon, respectively.

[1] S. W. Hawking and G. F. R. Ellis, *The Large Scale Structure of Space-Time* (Cambridge University Press, Cambridge, England, 1973).

[2] R. Casadio, Int. J. Mod. Phys. D **09**, 511 (2000); W. Piechocki and T. Schmitz, Phys. Rev. D **102**, 046004 (2020); V. Husain, J. G. Kelly, R. Santacruz, and E. Wilson-Ewing, arXiv:2109.08667.

[3] R. Penrose, in *Battelle Rencontres*, edited by C. de Witt and J. Wheeler (W.A. Benjamin, New York, 1968); R. A. Matzner, N. Zamorano, and V. D. Sandberg, Phys. Rev. D **19**, 2821 (1979); S. Chandrasekhar and J. B. Hartle, Proc. R. Soc. A **384**, 301 (1982); E. Poisson and W. Israel, Phys. Rev. Lett. **63**, 1663 (1989); E. Poisson and W. Israel, Phys. Rev. D **41**, 1796 (1990); A. Ori, Phys. Rev. Lett. **67**, 789 (1991); P. R. Brady and J. D. Smith, Phys. Rev. Lett. **75**, 1256 (1995); S. Hollands, R. M. Wald, and J. Zahn, Classical Quantum Gravity **37**, 115009 (2020).

[4] R. Penrose, Riv. Nuovo Cimento **1**, 252 (1969).

[5] R. Penrose, in *General Relativity, an Einstein Centenary Survey*, edited by S. W. Hawking and W. Israel (Cambridge University Press, Cambridge, England, 1979).

[6] P. R. Brady, I. G. Moss, and R. C. Myers, Phys. Rev. Lett. **80**, 3432 (1998).

[7] J. Bardeen, in *Proceeding of GR5*, edited by C. DeWitt and B. DeWitt (Gordon and Breach, Tbilisi, USSR, 1968), p. 174; I. Dymnikova, Gen. Relativ. Gravit. **24**, 235 (1992); E. Ayon-Beato and A. Garcia, Phys. Rev. Lett. **80**, 5056 (1998); K. A. Bronnikov, Phys. Rev. D **64**, 064013 (2001); S. A. Hayward, Phys. Rev. Lett. **96**, 031103 (2006); P. Nicolini, A. Smailagic, and E. Spallucci, Phys. Lett. B **632**, 547 (2006); C. Bambi and L. Modesto, Phys. Lett. B **721**, 329 (2013); C. A. R. Herdeiro and E. Radu, Phys. Rev. Lett. **112**, 221101 (2014); L. Balart and E. C. Vagenas, Phys. Rev. D **90**, 124045 (2014); Z. Y. Fan and X. Wang, Phys. Rev. D **94**, 124027 (2016); M. Azreg-Aïnou, Phys. Rev. D **90**, 064041 (2014); B. Toshmatov, B. Ahmedov, A. Abdujabbarov, and Z. Stuchlik, Phys. Rev. D **89**, 104017 (2014).

[8] A. Ashtekar and M. Bojowald, Classical Quantum Gravity **22**, 3349 (2005); H. M. Haggard and C. Rovelli, Phys. Rev. D **92**, 104020 (2015); J. Barrientos, A. Cisterna, N. Mora, and A. Viganò, arXiv:2202.06706.

[9] R. Casadio, arXiv:2103.00183; Universe **7**, 478 (2021).

[10] R. Casadio, A. Giugno, and A. Giusti, Phys. Lett. B **763**, 337 (2016).

[11] R. Casadio, A. Giugno, A. Giusti, and M. Lenzi, Phys. Rev. D **96**, 044010 (2017).

[12] G. Barnich, Gen. Relativ. Gravit. **43**, 2527 (2011).

[13] W. Mück, Can. J. Phys. **92**, 973 (2014).

[14] A. Giusti, S. Buffa, L. Heisenberg, and R. Casadio, Phys. Lett. B **826**, 136900 (2022).

[15] R. Casadio, Eur. Phys. J. C **82**, 10 (2022).

[16] X. Calmet, R. Casadio, S. D. H. Hsu, and F. Kuipers, Phys. Rev. Lett. **128**, 111301 (2022).

[17] J. Ovalle, R. Casadio, E. Contreras, and A. Sotomayor, Phys. Dark Universe **31**, 100744 (2021).

[18] R. L. Arnowitt, S. Deser, and C. W. Misner, Phys. Rev. **116**, 1322 (1959).

[19] R. P. Feynman, F. B. Morinigo, W. G. Wagner, and B. Hatfield, *Feynman Lectures on Gravitation* (Addison-Wesley Pub. Co., Reading, MA, 1995).

[20] R. P. Kerr and A. Schild, Proc. Symp. Appl. Math. **17**, 199 (1965); G. C. Debney, R. P. Kerr, and A. Schild, J. Math. Phys. (N.Y.) **10**, 1842 (1969).

[21] J. Ovalle, Phys. Rev. D **95**, 104019 (2017).

[22] J. Ovalle, Phys. Lett. B **788**, 213 (2019).

[23] V. N. Lukash and V. N. Strokov, Int. J. Mod. Phys. A **28**, 1350007 (2013).

[24] R. Casadio, O. Micu, and D. Stojkovic, J. High Energy Phys. 05 (2015) 096.

[25] R. Casadio, O. Micu, and D. Stojkovic, Phys. Lett. B **747**, 68 (2015).

[26] J. D. Bekenstein, Phys. Rev. D **7**, 2333 (1973).

[27] S. W. Hawking, Commun. Math. Phys. **43**, 199 (1975); **46**, 206 (1976).

[28] E. Contreras, J. Ovalle, and R. Casadio, Phys. Rev. D **103**, 044020 (2021).